Volume 60
Number 12
11 February 2024
Pages 1499–1652

ChemComm

Chemical Communications

rsc.li/chemcomm

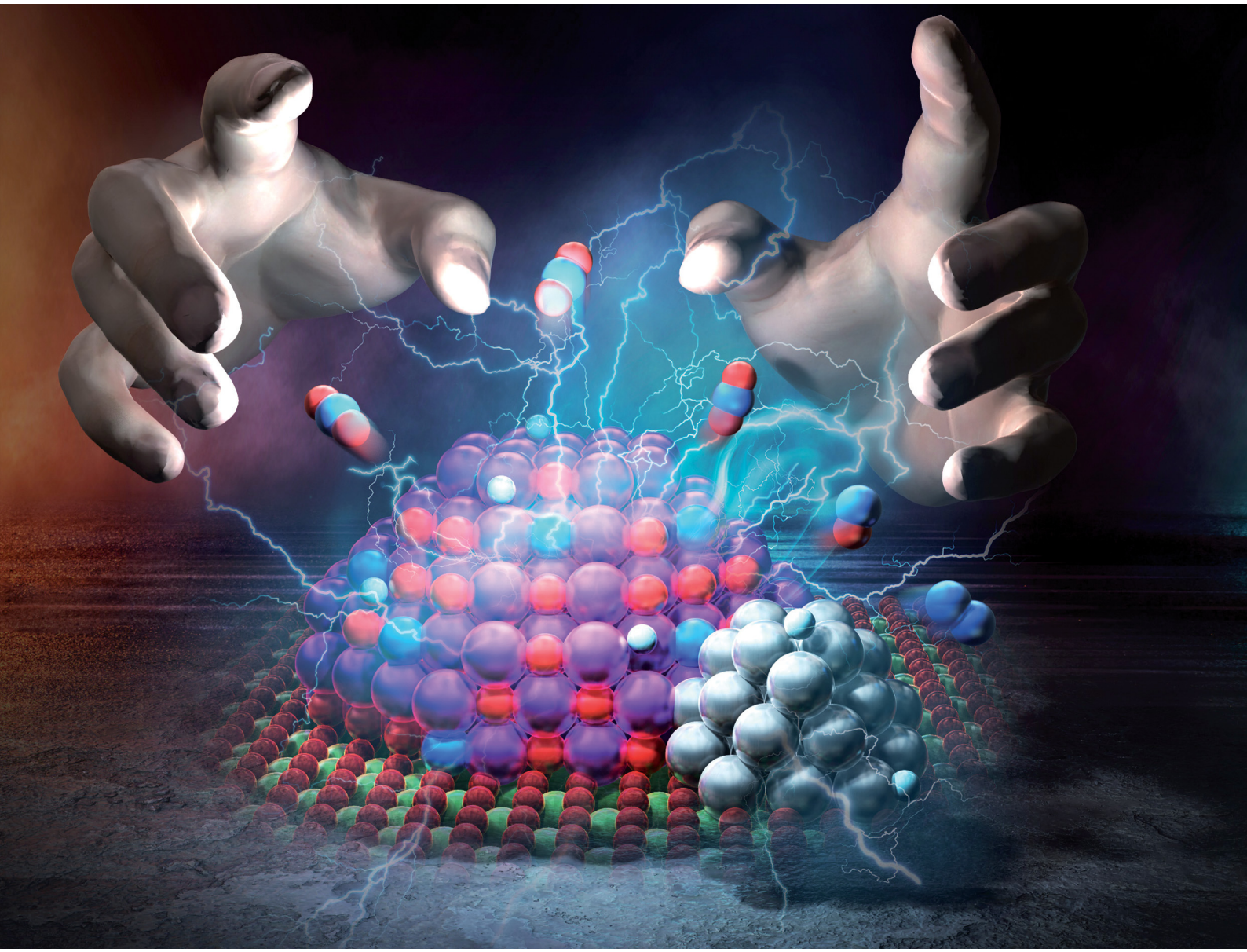

ISSN 1359-7345

ROYAL SOCIETY OF CHEMISTRY

COMMUNICATION

Ayaka Shigemoto, Yasushi Sekine *et al.*

Electric field-assisted NSR process for lean NO_x reduction at low temperatures

60 YEARS ANNIVERSARY

ChemComm

COMMUNICATION

View Article Online
View Journal | View Issue

Cite this: *Chem. Commun.*, 2024, **60**, 1563

Received 22nd October 2023,
Accepted 4th January 2024

DOI: 10.1039/d3cc05189g

rsc.li/chemcomm

Electric field-assisted NSR process for lean NO_x reduction at low temperatures†

Ayaka Shigemoto, *[a] Yuki Inoda,[a] Chihiro Ukai,[a] Takuma Higo, [a] Kohei Oka[b] and Yasushi Sekine *[a]

Lean-burn engines are gaining attention for their lower CO_2 emissions, higher thermal efficiency, and improved fuel economy compared to traditional combustion engines. However, they present some difficulty for reducing nitrogen oxides (NO_x) because of residual oxygen. To address this difficulty, NO_x storage reduction (NSR) system, which combines noble metals and NO_x adsorbents, is developed as a viable approach. But it requires cyclic operation, which adversely affects fuel efficiency. A novel approach proposed in this work is electric field-assisted lean NO_x reduction, which applies an electric field to the NSR catalyst during lean conditions. This innovation uses surplus vehicle electricity for exhaust purification, enhances hydrogen transfer, and improves NO_x reduction, even at low temperatures. Tests with a 3 wt% Pt–16 wt% BaO/CeO_2 catalyst demonstrate markedly higher NO_x conversion to N_2 (13.1% *vs.* 2.9% without an electric field). This process is effective with extended electric field exposure, doubling the conversion rate. Electric field-assisted lean NO_x reduction, by improving NSR technology, can enhance NO_x conversion efficiency, reduce emissions, and optimize fuel efficiency in lean-burn engines.

Lean-burn engines are attracting preference over stoichiometric combustion engines because of their lower CO_2 emissions, higher thermal efficiency, and better fuel economy.[1–3] However, classical three-way catalysts (TWCs) are ineffective at reducing nitrogen oxides (NO_x) because of the presence of residual oxygen (O_2) in the exhaust gases of lean burn engines. To overcome this difficulty, NO_x storage reduction (NSR) technology has attracted attention as a viable approach to remove NO_x from lean-burn engine exhaust.

Typical NSR catalysts combine noble metals (Pt, Pd, Rh) as active sites and alkali or alkaline earth metal oxides (Ba, K) as NO_x storage sites.[4–6] Conventional NSR catalysts work under cycling conditions. Under lean burn conditions, NO is oxidized by O_2 and is stored on the NSR catalyst surface in the form of nitrate (NO_3^-). In the following rich (oxygen-deprived) conditions, NO_x released from the surface is reduced to nitrogen (N_2) by reductants such as hydrogen (H_2), carbon monoxide and hydrocarbons.[7–9] However, conventional NSR technology requires complex cyclic operation with frequent switching between lean and rich states, resulting in unavoidably lower fuel efficiency.[10,11]

For this study, a new catalytic NSR process is proposed to reduce the adsorbed NO_x and to improve engine efficiency using H_2 in a lean burn state without switching to a rich combustion state after NO_x adsorption. This new concept is designated as electric field-assisted lean NO_x reduction, as an electric field is applied to the NSR catalyst during lean NO_x reduction. With the introduction of this technology, surplus electricity in the vehicle is useful for exhaust gas purification, which is part of energy management. Furthermore, the application of an electric field activates the reduction function of the supplied H_2 and simultaneously promotes hydrogen transfer. This effect promotes NO_x reduction, even at low temperatures. Our earlier reports have described that application of an electric field to the reaction enhances hydrogen transfer at the surface of the support.[12–15] In such heterogeneous catalysis under an electric field, the proton conductivity of the surface plays an important role, thereby enabling reaction pathways by collisions between H^+ on the catalyst support and adsorbates on the supported metal. We have already established a purification technique that allows very high NO conversion and N_2 selectivity, even at low temperatures, by the combination of catalyst and electric field.[16,17] In this study, a novel NSR process using a Pt–BaO/CeO_2 catalyst was shown to convert accumulated NO_x to N_2 efficiently, even at low temperatures of 423 K and under lean burn conditions.

Four NSR catalyst samples x wt% Pt–y wt% BaO/CeO_2 (x:y = 3:16, 0.5:16, 3:8, 0.5:8) in powder form were obtained from Umicore Shokubai Japan Co., Ltd. Fig. S1 (ESI†) shows the XRD patterns of four samples activated at 773 K for 30 min in 5% H_2/Ar (100 SCCM total flow rate). Here, CeO_2 was used as a support because, in the case of alumina and other materials, it is impossible

[a] *Department of Applied Chemistry, Waseda University, 3-4-1, Okubo, Shinjuku, Tokyo, 169-8555, Japan. E-mail: ayaka.shigemoto@nifty.com, ysekine@waseda.jp*
[b] *Isuzu Central Research Center, Fujisawa, Kanagawa, Japan*

† Electronic supplementary information (ESI) available. See DOI: https://doi.org/10.1039/d3cc05189g

to apply an electric field due to its insulating properties. Strong diffraction peaks attributed to CeO_2 and $BaCO_3$ were observed in all samples. In contrast, no diffraction for Pt and PtO_x was observed. This observation suggests that Pt is highly dispersed and not sufficiently large to be detected by XRD. Table S1 (ESI†) presents the results for the BET specific surface area and Pt particle size. Transmission electron microscopy (TEM) and HAADF images and EDX mapping of the four catalysts are exhibited in Fig. S2 (ESI†).

Catalytic activity tests were conducted in a fixed flow type quartz reactor at atmospheric pressure as shown in Fig. S3 (ESI†), and the procedure of activity tests is shown in Fig. S4 (ESI†). An electric field was applied with a power supply *via* stainless steel electrodes, contacting the catalyst bed (amount of fixed catalyst was 250 mg) on the upper and bottom sides. The results are plotted as the average of the three values obtained from the Q-mass (BELMass; MicrotracBEL Corp.).

The NO_x storage capacity of the four catalysts was measured at 573 K for 1 h with a continuous flow of 700 ppm NO and 8 vol% O_2 (200 sccm total flow rate). Also, Fig. S5 and Table S2 (ESI†) show that the 3 wt% Pt–16 wt% BaO/CeO_2 catalyst has the highest NO_x storage capacity of the four catalysts. As Fig. S2(a) (ESI†) shows, Pt and Ba on the 3 wt% Pt–16 wt% BaO/CeO_2 catalyst are highly dispersed on the CeO_2 support. There is no aggregation of Pt and Ba compared to the other three catalysts, indicating that Pt and Ba are highly interacting on the 3 wt% Pt–16 wt% BaO/CeO_2.

This result illustrates clearly that the NO_x storage capacity depends on the states of both Pt and Ba, which is in agreement with earlier studies pointing out that Pt in contact with Ba or in proximity to Ba is likely to be responsible for the high NO_x storage capacity.[7,18]

Lean NO_x reduction tests with and without an electric field were performed on the 3 wt% Pt–16 wt% BaO/CeO_2 catalyst with the highest NO_x storage capacity: 0.2 vol% H_2, 8 vol% O_2 and 10 vol% H_2O (200 sccm total flow rate) were flowed; the stored NO_x was reduced at 423 K for 1 h (200 sccm total flow rate). For 3 wt% Pt–16 wt% BaO/CeO_2 catalyst with and without the electric field, the conversion of stored NO_x to N_2 is presented in Fig. 1(a). For the catalytic reaction without the electric field, the conversion of NO_x to N_2 was only 2.9%. In contrast, when a 6-mA electric field was applied, high conversion of 13.1% was obtained even under lean burn conditions at the low temperature of 423 K. This result confirms that the electric field greatly promotes catalytic activity. In these tests, the catalyst bed temperature was directly measured using a thermocouple attached to the catalyst to confirm the effects of Joule heating induced by the applied direct current on the catalytic activity. Taking into account the Joule heating, lean NO_x reduction test was conducted even at 573 K (*i.e.* higher temperature) without the electric field. The conversion of NO_x to N_2 was only 3.5% shown in Fig. S6 (ESI†). Therefore, the high activity is not attributable to Joule heating. Furthermore, the distribution of nitrogen-containing species in the outlet gas of the 3 wt% Pt–16 wt% BaO/CeO_2 catalyst during lean NO_x reduction is shown in Fig. 1(b)–(d). N_2, NO, and NO_2 were detected as outlet gases, with no N_2O detected. Regarding NH_3 formation, quantitative

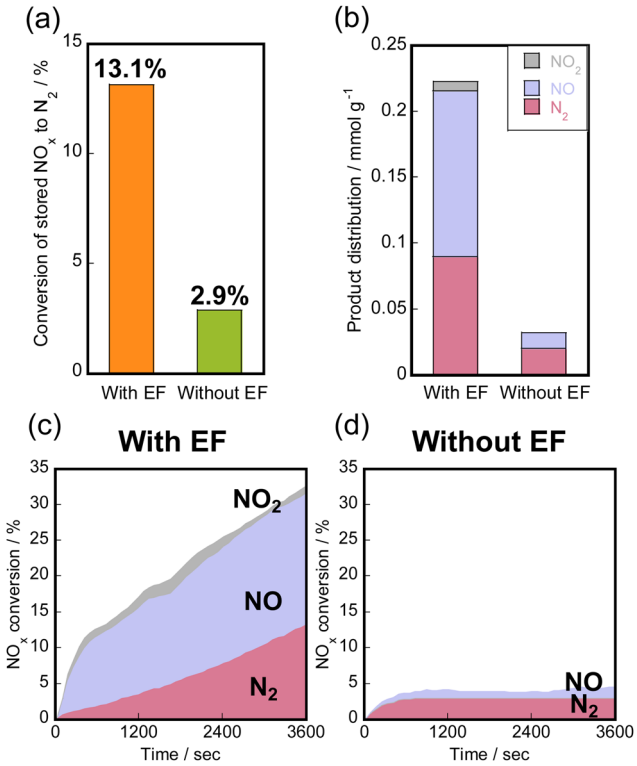

Fig. 1 Lean NO_x reduction over 3 wt% Pt–16 wt% BaO/CeO_2 with/without the electric field (EF): (a) conversion of NO_x to N_2, (b) NO_x and N_2 production amounts during one hour, and (c) and (d) the distribution of nitrogen-containing species in the outlet gas (calculated on nitrogen-base).

analysis was not possible because NH_3 was captured in the cold trap. However, the nitrogen balance demonstrated that NH_3 production was negligible (ESI† in Table S3 presents additional details). As presented in Fig. 1(c), the conversion of accumulated NO_x to N_2 increased linearly with the time course. By application of an electric field, the accumulated NO_x was reduced continuously to N_2. This reaction behaviour remained almost unchanged even when the electric field reduction time was doubled, resulting in the approximate doubling of NO_x to N_2 conversion from 13.1% to 29.1% (Fig. S7, ESI†). These results indicate that the continuous reduction of accumulated NO_x to N_2 is enhanced by the application of an electric field, even in a lean atmosphere.

In situ transmission infrared spectroscopy (TIRS) measurements were taken to investigate the behaviour of adsorbed NO_x in the reduction reaction using a 3 wt% Pt–16 wt% BaO/CeO_2 catalyst. The measurement procedure is shown in Fig. S8 (ESI†). Fig. S9 (ESI†) portrays the TIRS spectra of the surface species of the 3 wt% Pt–16 wt% BaO/CeO_2 catalyst when 700 ppm NO and 8 vol% O_2 were added, and when NO_x was adsorbed at 573 K. The bands at 1040 and 1270 cm^{-1} are shown in the TIRS spectra of the 3 wt% Pt–16 wt% BaO/CeO_2 catalyst. These bands are assigned respectively to monodentate and bidentate nitrates on the BaO phase.[19–21] Then, after dosing with 0.2 vol% H_2, 8 vol% O_2 and 5 vol% H_2O (100 sccm total flow rate) at 423 K in a 6-mA electric field, the absorbance of these

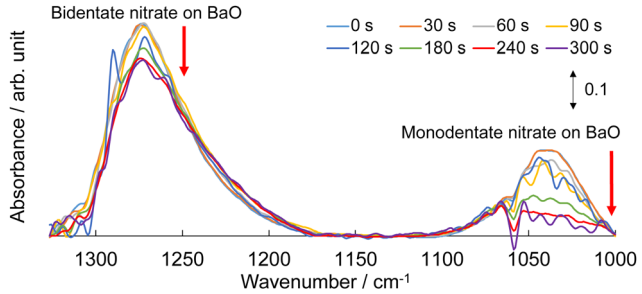

Fig. 2 Transmission infrared spectroscopy spectra during lean NO_x reduction over 3 wt% Pt–16 wt% BaO/CeO_2 with the electric field.

bands assigned to nitrate decreased, as presented in Fig. 2. Fig. S10 (ESI†) shows the TIRS spectra of 3 wt% Pt–16 wt% BaO/CeO_2 at 423 K without an electric field. A comparison of the normalized area of nitrate species with and without an electric field shows a marked increase in the decomposition rate of nitrate monovalent in the presence of an electric field, as shown in Fig. S11 (ESI†). This result shows good agreement with results obtained from the activity tests, indicating that greater removal of nitrate species from the surface is observed when an electric field is applied in a lean atmosphere.

It is generally considered that NO_x adsorbed at the Ba site is reduced to N_2 and NO by H_2 according to reactions (1) and (2).[22–24]

$$Ba(NO_3)_2 + 5H_2 \rightarrow N_2 + BaO + 5H_2O \quad (1)$$

$$Ba(NO_3)_2 + 3H_2 \rightarrow 2NO + BaO + 3H_2O \quad (2)$$

Findings obtained from the NO_x reduction reaction over 3 wt% Pt–16 wt% BaO/CeO_2 catalyst with and without an electric field clarify that more H_2 is consumed when the electric field is applied than when the field is not applied, as shown in Fig. S12 (ESI†). Fig. 3 portrays the breakdown of H_2 consumption during NO_x reduction, as calculated based on the stoichiometric ratio of H_2 to N_2 and NO in reactions (1) and (2). The total consumption of H_2 used to produce N_2 and NO in the electric field is 0.102 mmol (pink and purple areas). This figure shows close agreement with the 0.107 mmol of extra H_2 consumed during application of the electric field. This result suggests that the 3 wt% Pt–16 wt% BaO/CeO_2 catalyst can use H_2 to convert the accumulated NO_x to N_2 and NO, even in a lean atmosphere, by application of an electric field.

Several studies have investigated the mechanisms of reduction of accumulated NO_x. Reports of a few studies have included speculation that NO_x accumulated as nitrate spills over to available Pt sites and that NO and N_2 are released by the reductant, which has been termed reverse NO_x spillover.[25–28] Other reports have described that hydrogen spillover from Pt to the metal support occurs during the reduction of stored NO_x with H_2.[25,26,29,30] The proposed mechanism involves the activation of H_2 on Pt sites and the subsequent hydrogen spillover to nitrate ad-species on the storage component, mainly releasing NO. A possible scheme for NO_x storage and lean NO_x reduction on 3 wt% Pt–16 wt% BaO/CeO_2 is portrayed in Fig. 4, together with the electric field. During NO_x storage, NO_x is stored as nitrate ad-species on the BaO phase. During lean NO_x reduction, hydrogen is transferred from the Pt site to the storage component and reacts with the nitrate directly. Finally, the released NO_x reaches the Pt site, where NO_x is reduced to form N_2 and NO.

We showed earlier that the application of an electric field actively promotes hydrogen spillover/migration at the surface of the support in the low temperature range.[12–15] Indeed, we conducted lean NO_x reduction tests with a physical mixture of 3 wt% Pt/CeO_2 and 16 wt% $Ba(NO_3)_2/CeO_2$ catalyst. A schematic image of this catalyst is shown in Fig. S13 (ESI†). Fig. S14 (ESI†) portrays the protocol for activity tests. The nitrates were reduced to form NO only when applying the electric field, as illustrated in Fig. S15 and Table S4 (ESI†). These results clearly show that the nitrate decomposition occurs not only in close proximity to the Pt, but also further away from the Pt in the electric field. The NO_x reduction reaction hardly proceeded without hydrogen during the lean NO_x reduction in the electric field, indicating that the NO_x reduction resulted from hydrogen

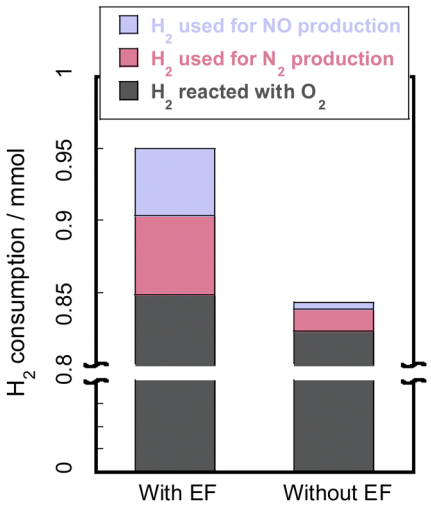

Fig. 3 Breakdown of H_2 consumption during lean NO_x reduction over 3 wt% Pt–16 wt% BaO/CeO_2 with and without the electric field.

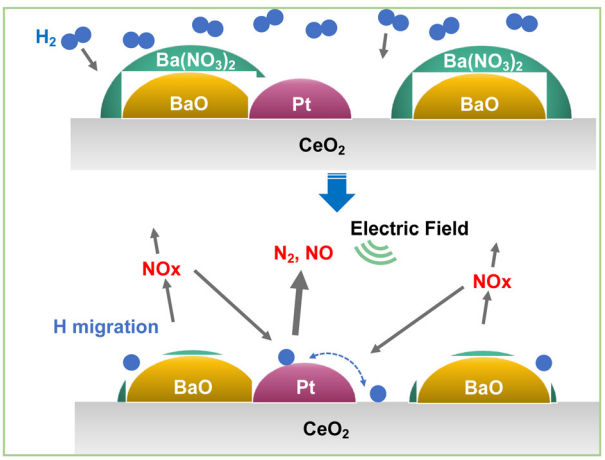

Fig. 4 Assumed reaction model for electric field-assisted lean NO_x reduction over 3 wt% Pt–16 wt% BaO/CeO_2.

spillover/migration due to the application of the electric field. Furthermore, to discuss the role of Pt for hydrogen spillover/migration, NO_x reduction tests were performed in the electric field using only 16 wt% $Ba(NO_3)_2/CeO_2$ catalyst without Pt. The amount of NO_x reduced was lower compared to the physical mixture of 3 wt% Pt/CeO_2 and 16 wt% $Ba(NO_3)_2/CeO_2$ catalyst, indicating that Pt is essential for hydrogen spillover/migration in the electric field (ESI† in Fig. S13–S15 and Table S4 presents additional details). An important role of the electric field in lean NO_x reduction under an electric field at low temperatures is to facilitate the activation and transfer of hydrogen species. Therefore, even under lean burn conditions, stored NO_x reduction can be achieved at the low temperature of 423 K.

The effect of applying an electric field to the catalyst for lean burn combustion, which has lower CO_2 emissions, higher thermal efficiency and better fuel economy than conventional internal combustion engines, was investigated by application of an electric field to the catalyst with the aim of operating NO_x storage and reduction (NSR) at lower temperatures. The proposed electric field-assisted lean NO_x reduction improved NO_x reduction at low temperatures using a small amount of excess electricity in (plug-in-) hybrid vehicles for exhaust purification and by promoting hydrogen transfer on the catalyst surface. The conversion of NO_x to N_2 was improved considerably when an electric field was applied using a 3 wt% Pt–16 wt% BaO/CeO_2 catalyst. The catalyst surface was investigated using infrared spectroscopy and reaction mechanisms was proposed. At present, the application of an electric field causes the desorption of absorbed NO as well as its conversion to nitrogen, but as the NO desorbed in this process has an increased outlet concentration, overall purification can also be achieved by effectively combining catalytic processes. Further development of the system is anticipated.

The authors thank Mr Koki Saegusa (Waseda University) for his great assistance in the TIRS measurements. The experiment of TEM was performed at the Joint Research Center for Environmentally Conscious Technologies in Materials Science (Grant no. JPMXP0723833151) at ZAIKEN, Waseda University. The author acknowledges the NSR powder supports from Umicore Shokubai Japan Co., Ltd.

Conflicts of interest

The authors have no conflict of interest.

References

1 S. Schemme, R. C. Samsun, R. Peters and D. Stolten, *Fuel*, 2017, **205**, 198–221.
2 N. Hooftman, M. Messagie, J. V. Mierlo and T. Coosemans, *Renewable Sustainable Energy Rev.*, 2018, **86**, 1–21.
3 S. A. Yashnik, *Catal. Ind.*, 2022, **14**, 283–297.
4 B. Pereda-Ayo, J. R. González-Velasco, R. Burch, C. Hardacre and S. Chansai, *J. Catal.*, 2012, **285**, 177–186.
5 L. Castoldi, R. Matarrese, L. Kubiak, M. Daturi, N. Artioli, S. Pompa and L. Lietti, *Catal. Today*, 2019, **320**, 141–151.
6 J. Luo, H. Xu, X. Liang, S. Wu, Z. Liu, Y. Tie, M. Li and D. Yang, *Res. Chem. Intermed.*, 2023, **49**, 2321–2357.
7 W. S. Epling, L. E. Campbell, A. Yezerets, N. W. Currier and J. E. Parks II, *Catal. Rev.: Sci. Eng.*, 2004, **46**, 163.
8 S. Matsumoto, *Catal. Today*, 2004, **90**, 183–190.
9 S. Roy and A. Baiker, *Chem. Rev.*, 2009, **109**, 4054–4091.
10 L. Xu and R. W. McCabe, *Catal. Today*, 2012, **184**, 83–94.
11 I. Heo, Y. W. You, J. H. Lee, S. J. Schmieg, D. Y. Yoon and C. H. Kim, *Environ. Sci. Technol.*, 2020, **54**, 8344–8351.
12 R. Inagaki, R. Manabe, Y. Hisai, Y. Kamite, T. Yabe, S. Ogo and Y. Sekine, *Int. J. Hydrogen Energy*, 2018, **43**, 14310–14318.
13 M. Torimoto, S. Ogo, Y. Hisai, N. Nakano, A. Takahashi, Q. Ma, J. G. Seo, H. Tsuneki, T. Norby and Y. Sekine, *RSC Adv.*, 2020, **10**, 26418–26424.
14 K. Murakami, Y. Tanaka, R. Sakai, Y. Hisai, S. Hayashi, Y. Mizutani, T. Higo, S. Ogo, J. G. Seo, H. Tsuneki and Y. Sekine, *Chem. Commun.*, 2020, **56**, 3365–3368.
15 Y. Sekine, *Faraday Discuss.*, 2023, **243**, 179–197.
16 A. Shigemoto, T. Higo, Y. Narita, S. Yamazoe, T. Uenishi and Y. Sekine, *Catal. Sci. Technol.*, 2022, **12**, 4450–4455.
17 Y. Omori, A. Shigemoto, K. Sugihara, T. Higo, T. Uenishi and Y. Sekine, *Catal. Sci. Technol.*, 2021, **11**, 4008–4011.
18 L. Castoldi, I. Nova, L. Lietti and P. Forzatti, *Catal. Today*, 2004, **96**, 43–52.
19 B. Caglar and D. Uner, *Catal. Commun.*, 2011, **12**, 450–453.
20 K. I. Hadjiivanov, *Catal. Rev.*, 2000, **42**, 102.
21 P. T. Fanson, M. R. Horton, W. N. Delgass and J. Lauterbach, *Appl. Catal., B*, 2003, **46**, 393–413.
22 P. Kočí, F. Plát, J. Štěpánek, Š. Bártová, M. Marek, M. Kubíček, V. Schmeißer, D. Chatterjee and M. Weibel, *Catal. Today*, 2009, **147**, S257–S264.
23 N. Maeda, A. Urakawa and A. Baiker, *J. Phys. Chem. C*, 2009, **113**, 16724–16735.
24 J. C. Martinez-Munuera, J. A. Giménez-Mañogil, R. Matarrese, L. Castoldi and A. García-García, *Appl. Sci.*, 2021, **11**, 5700.
25 Z. Liu and J. A. Anderson, *J. Catal.*, 2004, **224**, 18–27.
26 N. W. Cant, I. O. Y. Liu and M. J. Patterson, *J. Catal.*, 2006, **243**, 309–317.
27 L. Olsson, H. Persson, E. Fridell, M. Skoglundh and B. Andersson, *J. Phys. Chem. B*, 2001, **105**, 6895–6906.
28 A. Scotti, I. Nova, E. Tronconi, L. Castoldi, L. Lietti and P. Forzatti, *Ind. Eng. Chem. Res.*, 2004, **43**, 4522–4534.
29 I. Nova, L. Lietti and P. Forzatti, *Catal. Today*, 2008, **136**, 128–135.
30 M. Machida, D. Kurogi and T. Kijima, *J. Phys. Chem. B*, 2003, **107**, 196–202.

